Inorg. Chem. **2003**, *42*, 3245–3255

Rh(II) and Rh(I) Two-Legged Piano-Stool Complexes: Structure, Reactivity, and Electronic Properties

Felicia M. Dixon,[†] Martin S. Masar III,[†] Peter E. Doan,[†] Joshua R. Farrell,[†] Frederick P. Arnold Jr.,[†] Chad A. Mirkin,*[,†] Christopher D. Incarvito,[‡] Lev N. Zakharov,[‡] and Arnold L. Rheingold[‡]

Department of Chemistry and Center for Nanofabrication and Molecular Self-Assembly, Northwestern University, 2145 Sheridan Road, Evanston, Illinois 60208-3113, and Department of Chemistry and Biochemistry, University of Delaware, Newark, Delaware 19716

Received August 5, 2002

The ligand 1,4-bis[4-(diphenylphosphino)butyl]-2,3,5,6-tetramethylbenzene, **3**, was used to synthesize a mononuclear Rh(II) complex [(η^1:η^6:η^1-1,4-bis[4-(diphenylphosphino)butyl]-2,3,5,6-tetramethylbenzene)Rh][PF_6]$_2$, **6**$^+$, in a two-legged piano-stool geometry. The structural and electronic properties of this novel complex including a single-crystal EPR analysis are reported. The complex can be cleanly interconverted with its Rh(I) form, allowing for a comparison of the structural properties and reactivity of both oxidation states. The Rh(I) form **6** reacts with CO, *tert*-butyl isocyanide, and acetonitrile to form a series of 15-membered mononuclear cyclophanes [(η^1:η^1-1,4-bis[4-(diphenylphosphino)butyl]-2,3,5,6-tetramethylbenzene)Rh(CO)$_3$][PF_6] (**8**), [(η^1:η^1-1,4-bis[4-(diphenylphosphino)butyl]-2,3,5,6-tetramethylbenzene)Rh(CNC(CH$_3$)$_3$)$_2$][PF_6] (**10**), and [(η^1:η^1-1,4-bis[4-(diphenylphosphino)butyl]-2,3,5,6-tetramethylbenzene)Rh(CO)(CH$_3$CN)][PF_6] (**11**). The Rh(II) complex **6**$^+$ reacts with the same small molecules, but over shorter periods of time, to form the same Rh(I) products. In addition, a model two-legged piano-stool complex [(η^1:η^6:η^1-1,4-bis[3-(diphenylphosphino)propoxy]-2,3,5,6-tetramethylbenzene)Rh][$B(C_6F_5)_4$], **5**, has been synthesized and characterized for comparison purposes. The solid-state structures of complexes **5**, **6**, **6**$^+$, and **11** are reported. Structure data for **5**: triclinic; $P\bar{1}$; a = 10.1587(7) Å; b = 11.5228(8) Å; c = 17.2381(12) Å; α = 96.4379(13)°; β = 91.1870(12)°; γ = 106.1470(13)°; Z = 2. **6**: triclinic; $P\bar{1}$; a = 11.1934(5) Å; b = 12.4807(6) Å; c = 16.1771(7) Å; α = 81.935(7)°; β = 89.943(1)°; γ = 78.292(1)°; Z = 2. **6**$^+$: monoclinic; $P2(1)/n$; a = 11.9371(18) Å; b = 32.401(5) Å; c = 12.782(2) Å; β = 102.890(3)°; Z = 4. **11**: triclinic; $P\bar{1}$; a = 13.5476(7) Å; b = 13.8306(7) Å; c = 14.9948(8) Å; α = 74.551(1)°; β = 73.895(1)°; γ = 66.046(1)°; Z = 2.

Introduction

Mononuclear Rh(II) compounds are relatively rare when compared with the number of known Rh(I) and Rh(III) complexes.[1] Of the fifteen structurally characterized monomeric complexes, there are four predominant coordination geometries: square planar, octahedral, trigonal bipyramidal, and sandwich.[1c,2] We recently reported preliminary identification and characterization of a new class of mononuclear Rh(II) complexes in two-legged piano-stool geometries formed from symmetric bisphosphinoalkylarene ligands (Scheme 1).[3] This class of compounds was designed on the basis of a systematic study of the factors that control the stability of Rh(II) in this coordination environment that took into account ligand steric and electronic factors. The specific factors that contribute to the stabilization of rhodium(II) in this geometry are (1) an electron rich and sterically demand-

* To whom correspondence should be addressed. Fax: (847) 467-5123. E-mail: camirkin@chem.nwu.edu.
† Northwestern University.
‡ University of Delaware.

(1) (a) Cotton, F. A.; Waton, R. A. *Multiple Bonds Between Metal Atoms*; Wiley Interscience: New York, 1982. (b) Pandey, K. K. *Coord. Chem. Rev.* **1992**, *121*, 1. (c) Dewit, D. G. *Coord. Chem. Rev.* **1996**, *147*, 209.
(2) (a) Harlow, R. L.; Thorn, D. L.; Baker, R. T.; Jones, N. L. *Inorg. Chem.* **1992**, *31*, 993. (b) Connelly, N. G.; Emslie, D. J. H.; Geiger W. E.; Hayward, O. D.; Linehan, E. B.; Orpen A. G.; Quayle, M. J.; Rieger, P. H. *J. Chem. Soc., Dalton Trans.* **2001**, 670. (c) Haefner, S. C.; Dunbar, K. R.; Bender, C. *J. Am. Chem. Soc.* **1991**, *113*, 9540. (d) Paul, P.; Tyagi, B.; Bilakhiya, A. K.; Bhadbhade, M. M.; Suresh, E. *J. Chem. Soc., Dalton Trans.* **1999**, 2009. Collins, J. E.; Castellani, M. P.; Rheingold, A. L.; Miller, E. J.; Geiger, W. E.; Rieger, A. L.; Rieger, P. H. *Organometallics* **1995**, *14*, 1232.
(3) Dixon, F. M.; Farrell, J. R.; Doan, P. E.; Williamson, A.; Weinberger, D. A.; Mirkin, C. A.; Stern, C. L.; Incarvito, C. D.; Liable-Sands, L. M.; Zakharov, L. N.; Rheingold, A. L. *Organometallics* **2002**, *21*, 3091.

10.1021/ic0204981 CCC: $25.00
Published on Web 04/12/2003

Scheme 1

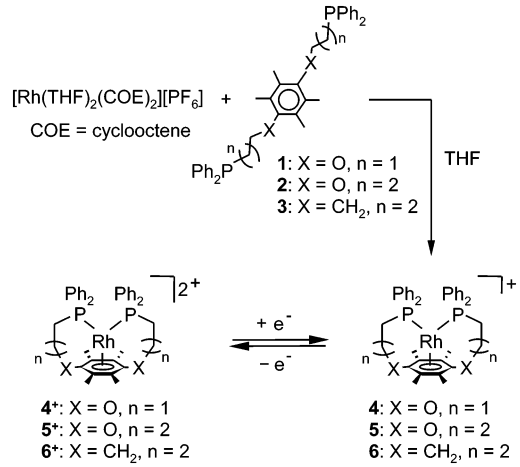

ing arene ring, (2) a symmetrically substituted arene ring, and (3) a flexible tether arm with phosphine connectivity that allows the complex to accommodate structural changes upon oxidation.[4]

Since there are very few examples of Rh(II) two-legged piano-stool complexes, little is known about their electronic structures, the ligand influences on such structures, and the reaction chemistry of complexes that make up this class of compounds. Herein, we report the synthesis and full characterization of a Rh(II) species in this geometry, a detailed solution and single-crystal EPR study, and theoretical studies aimed at understanding the metal contribution to the ground-state electronic configuration of the complex. In addition, we report the reactivity of both the Rh(I) and Rh(II) forms of this complex with respect to a variety of small molecules, including CO, *tert*-butyl isocyanide, and acetonitrile. Finally, we compare the properties of this complex with those of other Rh(II) two-legged piano-stool complexes that have been characterized in solution.

Experimental Section

General Procedures. Unless otherwise noted, all reactions were carried out under nitrogen using standard Schlenk techniques or in an inert atmosphere glovebox. Diethyl ether and tetrahydrofuran were dried and distilled over sodium/benzophenone. Methylene chloride and pentane were dried and distilled over calcium hydride. $[RhCl(COE)_2]_2$ (COE = cyclooctene) was prepared according to literature procedures.[5] CP grade carbon monoxide was purchased from Matheson Gas and passed through a column of Drierite prior to use. All other chemicals were obtained from commercial sources and used as received. NMR spectra were recorded on either a Varian Mercury 300 MHz or an Inova 500 MHz spectrometer. ^{1}H NMR signals are reported relative to residual proton resonances in deuterated solvents, and all signals are reported in parts per million with coupling constants in hertz. $^{31}P\{^1H\}$ NMR chemical shifts were measured relative to an external 85% H_3PO_4 standard. Fast-atom bombardment (FAB) and electron impact (EI) mass spectra were recorded using a Fisions VG 70-250 SE mass spectrometer, and electrospray (ES) mass spectra were recorded on a Micromass Quatro II triple quadrapole mass spectrometer. FT-IR spectra were recorded on a ThermoNicolet 670 spectrometer. Electrochemical measurements were carried out with a PINE AFRDE5 bipotentiostat/galvanostat using a Au electrode with a Pt mesh counter electrode and a silver wire quasi-reference electrode in a 0.1 M n-Bu_4NPF_6/CH_2Cl_2 solution. All electrochemical data were referenced using the Fc/Fc^+ ($Fc = (\eta^5\text{-}C_5H_5)Fe(\eta^5\text{-}C_5H_5)$) redox couple as an internal standard. Elemental analyses were obtained from Quantitative Technologies, Inc., Whitehouse, NJ.

Single-Crystal EPR Study. All EPR measurements were taken on a modified Varian E-4 X-band spectrometer. Frozen solution ($\mathbf{5}^+$, 19:1 CH_2Cl_2:$CHCl_3$; $\mathbf{6}^+$, CH_2Cl_2) EPR experiments were performed in a quartz finger dewar at 77 K. For the single-crystal experiments, a single crystal was mounted on a quartz fiber using Paratone and vacuum grease along the 010 face. Once the crystal was mounted, the faces were indexed using a Bruker Smart 1000 CCD diffractometer to verify its orientation. A simple goniometer was used in the single-crystal EPR experiments (accuracy $\pm$5 deg), and a nitrogen flow system was used to hold the temperature at 150 K. The field was calibrated using Mn(II)/MgO and diphenylpicrylhydrazyl (dpph) as standards. Field accuracy for the 2000 G sweeps reported was determined to be $\pm$3 G. The microwave frequency was measured with a frequency meter. Computer simulations of the frozen solution spectra of $\mathbf{5}^+$ and $\mathbf{6}^+$ were performed using the program QPOW.[6]

Theoretical Studies. Studies were performed on **6** and $\mathbf{6}^+$ with a substitution of methyl groups for phenyl rings on the phosphorus atoms in order to simplify the calculations by reducing the number of atoms present in the complexes. Undoubtedly, this change introduces steric and electronic differences between the calculated and the experimentally characterized structures. However, it has been shown that the electronic parameters for $PEtPh_2$ and $PEtMe_2$ are very similar.[7] The difference in the steric parameters between the methyl and phenyl versions of **6** and $\mathbf{6}^+$ can be estimated by examining the cone angles of $PEtPh_2$ (140°) and $PEtMe_2$ (approximately 122°).[7] The difference of nearly 20° is not negligible. However, the experimental crystal structures of **6** and $\mathbf{6}^+$ and the theoretical structures of the model complexes are very similar (vide infra), which suggests that the steric bulk of the phosphines does not have a large role in the determination of the optimized structures of these complexes. Geometries were optimized using Jaguar 4.2,[8] using the LACVP* effective core potentials and valence basis set, and the B3-GGA-II hybrid functional in C_2 symmetry. LACVP* employs ECP's only for the rhodium atoms, and the 6−31G* all-electron basis set for all other atoms. Structures were verified to be local minima on the potential surface by frequency analysis of the optimized structures. NBO analysis was performed using NBO 4.0[9] contained within Jaguar. The optimized geometries agree with the X-ray crystal structure for all bond distances (Rh(I), Rh−P = 2.29 Å (Δ = 0.04 Å), Rh−C_{av} 2.56 Å (Δ = 0.19 Å); Rh(II), Rh−P = 2.39 Å (Δ = 0.05 Å), Rh−C_{av} = 2.50 Å (Δ = 0.17 Å)).

X-ray Crystal Structure Determinations. Diffraction intensity data for complex **5** were collected using a Bruker Smart 1000 CCD diffractometer, and data for complexes **6**, $\mathbf{6}^+$, and **11** were collected

(4) (a) Singewald, E. T.; Slone, C. S.; Stern, C. L.; Mirkin, C. A.; Yap, G. P. A.; Liable-Sands, L. M.; Rheingold, A. L. *J. Am. Chem. Soc.* **1997**, *119*, 3048. (b) Harlow, R. L.; McKinney, R. J.; Whitney, J. F. *Organometallics* **1983**, *2*, 1839.
(5) Ent, A.; Onderdelinden, A. L. In *Reagents for Transition Metal Complex and Organometallic Syntheses*; Angelici, R. J., Ed.; John Wiley & Sons: New York, 1990; Vol. 28, pp 90−91.
(6) QPOW: EPR analysis software was furnished by the IL EPR research center, NIH Division of research resources Grant RR01811.
(7) Tolman, C. A. *Chem. Rev.* **1977**, *77*, 313.
(8) Schrodinger, Inc., 2002.
(9) NBO 4.0M: Glendeing, E. D.; Badenhoop, J. K.; Reed, A. E.; Carpenter, J. E.; Weinhold, F. *Theoretical Correction Program*; Bruker AXS: Madison, WI, 1996.

Table 1. Crystallographic Data for **5**, **6**, $\mathbf{6}^+$ and **11**

	5	**6**	$\mathbf{6}^+$	**11**
formula	$C_{43}H_{47}BF_4O_2P_2Rh$	$C_{44}H_{52}Cl_4F_6P_3Rh$	$C_{44}H_{52}Cl_4F_{12}P_4Rh$	$C_{47}H_{55}Cl_4F_6NOP_3Rh$
fw	847.5	1032.48	1177.45	1101.54
space group	$P\bar{1}$	$P\bar{1}$	$P2(1)/n$	$P\bar{1}$
cryst syst	triclinic	triclinic	monoclinic	triclinic
a, Å	10.1587(7)	11.1934(5)	11.9371(18)	13.5476(7)
b, Å	11.5228(8)	12.4807(6)	32.401(5)	13.8306(7)
c, Å	17.2381(12)	16.1771(7)	12.782(2)	14.9948(8)
α, deg	96.4379(13)	81.935(1)	90	74.551(1)
β, deg	91.1870(12)	89.943(1)	102.890(3)	73.895(1)
γ, deg	106.1470(13)	78.292(1)	90	66.046(1)
V, Å^3	1923.17(21)	2190.18(17)	4819.2(13)	2428.7(2)
Z	2	2	4	2
D(calc), g cm^{-3}	1.463	1.566	1.623	1.506
μ(Mo Kα), cm^{-1}	0.583	0.802	0.788	0.730
temp, K	153	120(2)	173(2)	128(2)
radiation		Mo Kα ($\lambda = 0.71073$ Å)		
$R(F)$, %[a]	5.9	5.19	4.45	6.62
$R(\omega F^2)$, %[b]	6.7	14.62	13.70	18.45

[a] $R = \sum||F_o| - |F_c||/\sum|F_o|$. [b] $R(\omega F^2) = \{\sum[\omega(F_o^2 - F_c^2)^2]/\sum[\omega(F_o^2)^2]\}^{1/2}$; $\omega = 1/\sigma^2(F_o^2) + (aP)^2 + bP]$, $P = [2F_c^2 + \max(F_o,0)]/3$.

with a Bruker Smart Apex CCD diffractometer. Crystal, data collection, and refinement parameters are given in Table 1. The space groups for complexes **5**, **6**, and **11** were chosen on the basis of intensity statistics, and the space group for $\mathbf{6}^+$ was determined from systematic absences in the diffraction data. The structures were solved using direct methods (**5**, **6**, $\mathbf{6}^+$) or the Patterson function (**11**), completed by subsequent difference Fourier syntheses, and refined by full matrix least-squares procedures on reflection intensities (F^2). SADABS[10] absorption corrections were applied to all data; in complexes **5** ($T_{min}/T_{max} = 0.87$), **6** ($T_{min}/T_{max} = 0.86$), $\mathbf{6}^+$ ($T_{min}/T_{max} = 0.91$), and **11** ($T_{min}/T_{max} = 0.85$). Besides the main molecules in the crystal structure of **5** there is one benzene molecule, and in the crystal structures of complexes **6** and **11** there are two CH_2Cl_2 molecules. In the crystal structure of **6**, the solvate molecules are disordered, and the program SQUEEZE[11] was used to treat them. Corrections of the X-ray data for **6** by SQUEEZE (170 electrons/cell) were close to the required values (168 electrons/cell). Non-hydrogen atoms in all structures were refined with anisotropic displacement coefficients, and hydrogen atoms were treated as idealized contributions, with thermal parameters defined as 1.2 that of the parent atom. Data were collected and processed using the Bruker Smart-NT and SAINT-NT programs. For complex **5**, all calculations were performed using the teXsan crystallographic software package of Molecular Structure Corporation. Software and source scattering factors for **6**, $\mathbf{6}^+$, and **11** are contained in the SHELXTL[12] (5.10) program package (G.Sheldrick, Bruker XRD, Madison, WI). Crystallographic data (excluding structure factors) for the structures in this paper have been deposited with the Cambridge Crystallographic Data Centre as supplementary publications CCDC-173487 (**5**), CCDC-175054 (**6**), CCDC-173489 ($\mathbf{6}^+$), and CCDC-189166 (**11**). Copies of the data can be obtained, free of charge, on application to CCDC, 12 Union Road, Cambridge CB2 1EZ, U.K. (Fax, +44 1223 336033; or e-mail, deposit@ccdc.cam.ac.uk).

Synthesis of 1,4-Bis(4-chlorobutyl)-2,3,5,6-tetramethylbenzene. A flask equipped with a condenser was charged with diiododurene (1 g, 2.6 mmol) and $Pd(PPh_3)_4$ (0.45 g, 15 mol %). An excess of a 0.5 M THF solution of 4-chlorobutylzinc bromide (~20 mL) was cannula transferred to the reaction mixture and refluxed at 80 °C for 12 h under a nitrogen bubbler. Aqueous ammonium chloride (20 mL) was added to the resulting brown solution to quench any remaining zinc. The resulting crude product was extracted using diethyl ether to yield an orange solution. The solution was dried with $CaCl_2$, filtered, and then washed with diethyl ether. Pure product (0.26 g, 31%) was obtained via column chromatography (1 in. diameter, 2 in. of neutral alumina) by collecting the second band with 1:4 ethyl acetate:hexanes as the eluent. ^{1}H NMR ($CDCl_3$): 1.63 (m, CH_2CH$_2$(C$_6$(CH$_3$)$_4$), 4H), 1.93 (m, CH$_2$CH_2Cl, 4H), 2.25 (s, C$_6$(CH_3)$_4$, 12H), 2.69 (m, CH_2(C$_6$(CH$_3$)$_4$), 4H), 3.62 (t, CH_2Cl, $J_{H-H} = 6.6$ Hz, 4H). ^{13}C{^{1}H} NMR ($CDCl_3$): δ 16.6 (s, C$_6$(*C*H$_3$)$_4$), 27.1 (s, *C*H$_2$CH$_2$(C$_6$(CH$_3$)$_4$), 30.0 (s, *C*H$_2$(C$_6$(CH$_3$)$_4$), 33.1 (s, *C*H$_2$CH$_2$Cl), 45.0 (s, *C*H$_2$Cl), 132.3 (s, *C*$_{6o}$(CH$_3$)$_4$), 136.4 (s, *C*$_{6i}$(CH$_3$)$_4$). HRMS (EI): calcd = 314.15676, found = 314.15663 *m*/*z*. Elemental anal. for $C_{18}H_{28}Cl_2$: calcd, % C = 68.56, % H = 8.95; found, % C = 68.52, % H = 8.86. Mp = 92−93 °C.

Synthesis of 1,4-Bis[4-(diphenylphosphino)butyl]-2,3,5,6-tetramethylbenzene (3). A THF solution of $KPPh_2$ (0.5M, 1.3 mL, 0.653 mmol) was added dropwise via a syringe to a flask containing a THF solution (20 mL) of the chloro precursor described above (100 mg, 0.318 mmol). The resulting mixture was stirred vigorously under nitrogen for 2 h, at which time the solvent was removed in vacuo. An extraction using CH_2Cl_2 and H_2O yielded a white solid, which was flashed through Celite with CH_2Cl_2 to remove any residual salt. Pure **3** was obtained as a white solid after washing of the solid with a minimal amount of EtOH (30 mL) followed by cannula filtration, (0.167 g, 85%). ^{1}H NMR (CD_2Cl_2): 1.65 (m, PCH$_2$CH_2 and PCH$_2$CH$_2$CH_2, 8H), 2.17 (m, PCH_2, 4H), 2.25 (s, C$_6$(CH_3)$_4$, 12H), 2.69 (m, CH_2(C$_6$(CH$_3$)$_4$), 4H), 7.39−7.49 (m, P(C$_6H_5$)$_2$, 20H). ^{13}C{^{1}H} NMR (CD_2Cl_2): 16.6 (s, C$_6$(*C*H$_3$)$_4$), 26.6 (d, $J_{C-P} = 12.5$, PCH$_2$*C*H$_2$), 27.9 (d, $J_{C-P} = 9.1$, PCH$_2$CH$_2$*C*H$_2$), 30.6 (s, *C*H$_2$(C$_6$(CH$_3$)$_4$), 31.4 (d, $J_{C-P} = 10.2$, P*C*H$_2$), 128.5 (s, P(C$_{6p}$H$_5$)$_2$), 128.6 (d, $J_{C-P} = 3.67$, P(C$_{6m}$H$_5$)$_2$), 132.1 (s, *C*$_{6o}$(CH$_3$)$_4$, 132.7 (d, $J_{C-P} = 14.6$, P(C$_{6o}$H$_5$)$_2$), 136.7 (s, *C*$_{6i}$(CH$_3$)$_4$), 138.9 (d, $J_{C-P} = 10.2$, P(C$_{6i}$H$_5$)$_2$). ^{31}P {^{1}H} NMR (CD_2Cl_2): −15.3 (s). HRMS (EI): calcd = 614.32312, found = 614.32304 *m*/*z*. Elemental anal. for $C_{42}H_{48}P_2$: calcd, % C = 82.05, % H = 7.87; found, % C = 82.32, % H = 7.76. Mp = 114−116 °C.

Synthesis of [(η^1:η^6:η^1-1,4-Bis[3-(diphenylphosphino)propoxy]-2,3,5,6-tetramethylbenzene)Rh][B(C$_6$F$_5$)$_4$] (5). In a glovebox, $[RhCl(COE)_2]_2$ (40.0 mg, 0.111 mmol) and $AgBF_4$ (22 mg, 0.113 mmol) were stirred in 3 mL of CH_2Cl_2 for 1 h. The resulting

(10) Sheldrick, G. M. *SADABS (2.01), Bruker/Siemens Area Detector Absorption Correction Program*; Bruker AXS: Madison, WI, 1998.
(11) Van der Sluis, P.; Spek, A. L. *Acta Crystallogr., Sect. A* **1990**, *A46*, 194.
(12) G. Sheldrick, Bruker XRD, Madison, WI.

reaction mixture was filtered through Celite to remove a light gray precipitate, which was presumably AgCl. The filtrate was then reacted with $LiB(C_6F_5)_4$ (105 mg, 0.138 mmol), filtered through Celite, and diluted with 125 mL of THF. A solution of 1,4-bis[3-(diphenylphosphino)propoxy]-2,3,5,6-tetramethylbenzene (68.6 mg, 0.111 mmol) in 125 mL of THF was added dropwise at −78 °C over 2 h to the reaction mixture. The solution was warmed to room temperature over 1 h and then refluxed for 3 days. At this elevated temperature, the solvent was removed in vacuo to yield an orange powder. Redissolving the powder in CH_2Cl_2 and layering with Et_2O removed the remaining COE and afforded **5** (yield = 58%, 0.090 g, 0.0064 mmol). Recrystallization from CH_2Cl_2/C_6H_6 afforded thin red blades of **5**, which were characterized by X-ray crystallography. ^{1}H NMR (CD_2Cl_2): 1.38−1.50 (bm, 4H, $CH_2CH_2CH_2$), 2.35−2.42 (bm, 4H, CH_2P), 2.55 (s, 12H, $C_6(CH_3)_4$), 4.00 (t, 4H, CH_2O, J_{H-H} = 5.7), 7.05−7.20 (m, 20H, $P(C_6H_5)_2$). $^{31}P\{^1H\}$ NMR (CD_2Cl_2): δ 18.1 (d, J_{Rh-P} = 204). MS (FAB^+): $[M]^+$ calcd = 721.1872, exptl = 721.1879 *m/z*. Elemental anal. for $C_{64}H_{44}P_2O_2RhBF_{20}\cdot CCH_2Cl_2$: calcd, % C = 52.55, % H = 3.12; found, % C = 52.22, % H = 3.79.

Synthesis of [(η^1:η^6:η^1-1,4-Bis[3-(diphenylphosphino)propoxy]-2,3,5,6-tetramethylbenzene)Rh][$B(C_6F_5)_4$][BF_4] (5^+). Compound **5** (10.0 mg, 7.14×10^{-6} mol) and $AgBF_4$ (1.4 mg, 7.14×10^{-6} mol) were reacted in 3 mL of CH_2Cl_2 for 12 h in a glovebox. The resulting reaction mixture was filtered through Celite, and the solvent was removed in vacuo yielding $\mathbf{5}^+$ as a red-brown solid (yield = 94%, 0.010 g, 6.72×10^{-6} mol). A saturated CH_2Cl_2 solution (10 mL) of $\mathbf{5}^+$ was mixed with Et_2O (25 mL) to precipitate a red-brown solid. The solid was collected on a Celite filter and then dissolved in CH_2Cl_2 (20 mL). The solvent was removed in vacuo to give $\mathbf{5}^+$ as a red-brown solid, which allowed for elemental analysis. ^{1}H NMR (CD_2Cl_2): 9.4 (b, unassignable), 5.9 (b, unassignable). $^{31}P\{^1H\}$ NMR (CD_2Cl_2): no signal. MS(ES): $[M - BF_4]^+$ calcd = 1400.2, exptl = 1400.3 *m/z*, $[M]^{2+}$ calcd = 360.6, exptl = 360.2 *m/z*. Elemental anal. for $C_{64}H_{44}P_2O_2RhB_2F_{24}$: calcd % C = 51.68, % H = 2.98; found: % C = 51.60, % H = 3.24.

Synthesis of [(η^1:η^6:η^1-1,4-Bis[4-(diphenylphosphino)butyl]-2,3,5,6-tetramethylbenzene)Rh][PF_6] (6). In a glovebox, $[RhCl(COE)_2]_2$ (40.0 mg, 0.111 mmol) and $AgPF_6$ (28 mg, 0.111 mmol) were reacted in 3 mL of CH_2Cl_2 for 30 min. The resulting reaction mixture was filtered through Celite, which removed a light gray precipitate, and then diluted with 30 mL of THF. A solution of **3** (68 mg, 0.111 mmol) in 30 mL of THF was added dropwise over 30 min at −78 °C to the filtrate. The solution was warmed to room temperature over 1 h followed by heating at 50 °C for 4 h. The solvent was removed in vacuo at 50 °C to yield an orange solid. Compound **6** was precipitated as a deep red solid from a concentrated CH_2Cl_2 solution with pentane (18 mg, 20%). X-ray grade crystals of **6** were grown by slow diffusion of pentane into a CH_2Cl_2 solution saturated with **6**. ^{1}H NMR(CD_2Cl_2): 1.665 (bm, $CH_2CH_2(C_6(CH_3)_4)$, 4H), 2.112 (bm, $PCH_2CH_2CH_2$, 8H), 2.202 (s, $C_6(CH_3)_4$, 12H), 2.700 (bm, $CH_2(C_6(CH_3)_4)$, 4H), 7.090−7.215 (m, $P(C_6H_5)_2$, 20H). ^{31}P {^{1}H} NMR (CD_2Cl_2): 28.0 (d, J_{Rh-P} = 204). MS(ES): $[M]^+$ calcd = 717.2, exptl = 717.2 *m/z*. Elemental anal. for $C_{42}H_{48}F_6P_3Rh$: calcd, % C = 58.48, % H = 5.61; found, % C = 58.30, % H = 5.74.

Synthesis of [(η^1:η^6:η^1-1,4-Bis[4-(diphenylphosphino)butyl]-2,3,5,6-tetramethylbenzene)Rh][PF_6]$_2$ (6^+). As with **5**, complex **6** (10 mg, 0.0116 mmol) was combined with excess $AgPF_6$ in CH_2Cl_2 (3 mL) and stirred vigorously for 30 min followed by filtration to remove a Ag^0 precipitate, yielding a yellow-brown solution. Removal of solvent yields $\mathbf{6}^+$ as a yellow-brown solid (yield = 90%, 0.0105 g, 0.0104 mmol). Single crystals of $\mathbf{6}^+$ suitable for an X-ray diffraction analysis were grown by slow vapor diffusion of diethyl ether into a CH_2Cl_2 solution saturated with $\mathbf{6}^+$ at 0 °C.^{1}H NMR(CD_2Cl_2): 1.78 (b, unassignable), 2.11−2.25 (b, unassignable), 2.709 (b, unassignable), 7.7 (bm, $P(C_6H_5)_2$). $^{31}P\{^1H\}$ NMR (CD_2Cl_2): no signal. Elemental anal. for $C_{42}H_{48}F_{12}P_4Rh$: calcd, % C = 50.06, % H = 4.80; found, % C = 50.00, % H = 4.95. Despite attempts using several different techniques, mass spectral analysis aimed at identifying the 2+ ion was unattainable due to the reduction of $\mathbf{6}^+$ to **6** during ionization.

Synthesis of [(η^1:η^1-1,4-Bis[4-(diphenylphosphino)butyl]-2,3,5,6-tetramethylbenzene)Rh$(CO)_3$][PF_6] (8). In a typical reaction, a red CH_2Cl_2 (1 mL) solution of **6** (10 mg, 0.01159 mmol) was charged with CO for 4 h in a Teflon valved air-free NMR tube. The reaction vessel was kept at room temperature for 40 days, with periodic monitoring by $^{31}P\{^1H\}$ NMR spectroscopy, before the complete conversion to **8** was observed. The resulting yellow solution was determined to contain **8** by the following methods. ^{1}H NMR (CD_2Cl_2): 1.28 (b, $Ph_2PCH_2CH_2CH_2CH_2$, 4H), 1.90 (b, $Ph_2PCH_2CH_2CH_2$, 4H), 2.14 (s, $C_6(CH_3)_4$, 12H), 2.49 (b, $Ph_2PCH_2CH_2$, 4H), 3.00 (b, $CH_2(C_6(CH_3)_4)$, 4H), 7.47−7.61 (m, $(C_6H_5)_2P$, 20H). $^{31}P\{^1H\}$ NMR (CD_2Cl_2): 30.4 (d, J_{Rh-P} = 72). FT-IR (CH_2Cl_2): ν_{CO} = 2023 (s), 2034 (s), and 2091 (w) cm^{-1}. MS (ES): $[M - 3CO]^+$ calcd = 717.2, found = 717.0. The lability of the CO ligands prevented elemental combustion analysis.

Synthesis of [*trans*-(η^1:η^1-1,4-Bis[4-(diphenylphosphino)butyl]-2,3,5,6-tetramethylbenzene)Rh$(CO)_2$][PF_6] (9a) and [*cis*-(η^1:η^1-1,4-Bis[4-(diphenylphosphino)butyl]-2,3,5,6-tetramethylbenzene)Rh$(CO)_2$][PF_6] (9b). The synthesis of complex **9a** is identical to the synthesis for **8** except the reaction mixture is heated at 51 °C for 3 days. Complex **9b** is observed as an unstable intermediate that transforms into **9a** and cannot be isolated. **9a**: ^{1}H NMR (CD_2Cl_2) 1.52 (b, $Ph_2PCH_2CH_2CH_2CH_2$, 4H), 1.68 (b, $Ph_2PCH_2CH_2CH_2$, 4H), 2.18 (s, $C_6(CH_3)_4$, 12H), 2.58 (b, $Ph_2PCH_2CH_2$ and $CH_2(C_6(CH_3)_4)$, 8H), 7.44−7.67 (m, $(C_6H_5)_2P$, 20H); $^{31}P\{^1H\}$ NMR (CD_2Cl_2) 23.9 (d, J_{Rh-P} = 121). **9b**: $^{31}P\{^1H\}$ NMR (CD_2Cl_2) 25.3 (J_{Rh-P} = 105 Hz). The FT-IR spectrum was unassignable owing to the presence of **8** in the samples. MS and EA were not possible due to the lability of the CO and the presence of **8**.

Synthesis of [(η^1:η^1-1,4-Bis[4-(diphenylphosphino)butyl]-2,3,5,6-tetramethylbenzene)Rh$(CNC(CH_3)_3)_2$][PF_6] (10). To a CH_2Cl_2 (1 mL) solution of **6** (10 mg, 0.01159 mmol) was added 2 equiv of *tert*-butyl isocyanide (2.6 μL, 0.02318 mmol) followed by heating at 45 °C for 3 days, resulting in the quantitative formation of the diisocyanide adduct, **10**, as determined by NMR spectroscopy. ^{1}H NMR (CD_2Cl_2): 0.86 (s, $CNC(CH_3)_3$, 18H), 1.28 (b, $Ph_2PCH_2CH_2CH_2CH_2$, 4H), 1.90 (b, $Ph_2PCH_2CH_2CH_2CH_2$, 4H), 2.14 (s, $C_6(CH_3)_4$, 12H), 2.49 (b, $Ph_2PCH_2CH_2CH_2$, 4H), 3.00 (b, $CH_2(C_6(CH_3)_4)$, 4H), 7.47−7.61 (m, $(C_6H_5)_2P$, 20H). $^{31}P\{^1H\}$ NMR (CD_2Cl_2): 23.6 (d, J_{Rh-P} = 123). FT-IR (CH_2Cl_2): ν_{NC} = 2135 cm^{-1}. MS (ES): $[M]^+$ calcd = 883.4, found= 883.1. Elemental combustion analysis was not possible due to the lability of the isocyanide ligands upon evacuation.

Synthesis of [(η^1:η^1-1,4-Bis[4-(diphenylphosphino)butyl]-2,3,5,6-tetramethylbenzene)Rh(CO)(CH_3CN)][PF_6] (11). Excess CH_3CN was added to a CD_2Cl_2 solution of **6** (10 mg, 0.01159 mmol) in a Teflon sealed air-free NMR tube followed by charging with CO (1 atm) for 30 min. The reaction mixture was heated at 40 °C for 3 days, which resulted in the quantitative formation of **11**, as determined by NMR spectroscopy. Compound **11** was characterized in solution and by mass spectrometry. Single crystals of **11** suitable for an X-ray diffraction analysis were grown by slow diffusion of pentane into a CH_2Cl_2 solution saturated with **11** at

room temperature. ^{1}H NMR (CD_2Cl_2): 1.28 (b, $Ph_2PCH_2CH_2CH_2$-CH_2, 4H), 1.80 (b, $Ph_2PCH_2CH_2CH_2CH_2$, 4H), 2.14 (s, $C_6(CH_3)_4$, 12H), 2.40 (b, $Ph_2PCH_2CH_2$, 4H), 2.93 (b, $CH_2(C_6(CH_3)_4)$, 4H), 7.52 (b, $(C_6H_5)_2P$, 20H). $^{31}P\{^1H\}$ NMR (CD_2Cl_2): 27.2 (d, $J_{Rh-P} = 97$). FT-IR (CH_2Cl_2): $\nu_{CO} = 1976$ (s), $\nu_{CH3CN} = 2218$ (s) cm^{-1}. MS (ES): [M$^+$] calcd = 786.3, found = 786.1. Elemental combustion analysis was not possible for this compound owing to the lability of the ligands upon evacuation.

Reactivity of 6^+ with Small Molecules. In a typical reaction, a CH_2Cl_2 solution of $\mathbf{6}^+$ was charged with CO or a stoichiometric amount of the ancillary ligand. In the case of CO and *tert*-butyl isocyanide, the brown solution turns yellow upon reaction at 51 °C and results in the formation of the reduction/substitution products **8** (12 h) and **10** (24 h), respectively. See syntheses of complexes **8** and **10** for characterization. Reaction of $\mathbf{6}^+$ with CO and acetonitrile resulted in decomposition with no identifiable products.

Results and Discussion

Synthesis and Characterization of Mononuclear Rh(I) Complexes 5 and 6. Previous studies in our group with mononuclear two-legged piano-stool complexes suggest that an ideal ligand framework for the stabilization and isolation of mononuclear Rh(II) with this geometry consists of a symmetrically substituted arene with two tethered phosphine moieties, where the arene is sterically protected with electron-donating alkyl moieties and the tethers are long enough to accommodate structural changes upon complex oxidation. As a result, bis(phosphinoalkyl)aryl ligands **1**−**3** were designed and synthesized. Ligands **1** (1,4-bis[4-(diphenylphosphino)ethoxy]-2,3,5,6-tetramethylbenzene**)** and **2** (1,4-bis[4-(diphenylphosphino)propoxy]-2,3,5,6-tetramethylbenzene) have been previously reported,[13] while ligand **3**, 1,4-bis[4-(diphenylphosphino)butyl]-2,3,5,6-tetramethylbenzene, was synthesized in two steps via a standard zinc-mediated coupling reaction[14] followed by nucleophilic substitution. Ligand **3** is a moderately air-sensitive white solid that has been characterized by ^{1}H and $^{31}P\{^1H\}$ NMR spectroscopies, mass spectrometry, combustion analysis, and melting point determination. Complex **4** was prepared via literature procedures, and **5** and **6** were prepared from ligands **2** and **3** and the appropriate Rh(I) precursor.[13] Compound **5** is obtained in almost 60% yield after refluxing the solution for 3 days, while **6** is formed in only 20% yield after 4 h of heating at 50 °C. The difference in reactivity is attributed to the ether groups in ligand **2**, which can template the formation of **5** through a binuclear intermediate (Scheme 2). Complex **5** is the thermodynamic product of a high-yielding reaction pathway that initially results in the formation of a binuclear intermediate **7**, which cleanly condenses into mononuclear compound **5**.[13] The reaction to form complex **6**, which involves a phosphinoalkylarene ligand without ether moieties, is prone to the formation of oligomers and polymers, which substantially lowers the yield of the target complex. Changes in dilution (3-fold) and temperature (room temperature to refluxing THF) were attempted to bypass the formation of the oligomers, but without the ethers acting as intramolecular templating agents, the formation of oligomers was unavoidable under the conditions explored. Complexes **5** and **6** have been characterized by ^{1}H and $^{31}P\{^1H\}$ NMR spectroscopy, mass spectrometry, elemental analysis, and X-ray diffraction analyses. The $^{31}P\{^1H\}$ NMR spectra of **5** and **6** each exhibit single resonances (**5**, δ 18.1, d, $J_{Rh-P} =$ 204 Hz; **6**, δ 28.0, d, $J_{Rh-P} = 204$ Hz) that are characteristic of complexes with two-legged piano-stool geometries about the rhodium(I) center.

Scheme 2

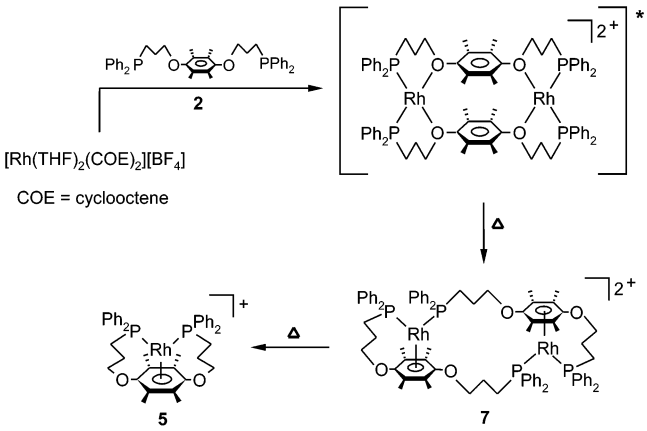

The relative kinetic and thermodynamic stabilities of the Rh(II) complexes can be determined by assessing the reversibility of the oxidation/reduction wave as a function of scan rate and the corresponding $E_{1/2}$ values, respectively. Therefore, cyclic voltammetry studies were conducted on **4**−**6** in CH_2Cl_2 at room temperature. All three complexes exhibit reversible one electron oxidation waves at all measured scan rates (1 mV/s to 1 V/s); a cyclic voltammogram of **6** at a sweep rate of 400 mV/s is provided as a representative example of the electrochemical stability of these complexes (Figure 1). The $E_{1/2}$ values for **4**−**6** are 560, 528, and 410 mV vs Fc/Fc$^+$ [Fc = (η^5-C_5H_5)−Fe−(η^5-C_5H_5)], respectively. Comparing the $E_{1/2}$ value for **5** with the $E_{1/2}$ for complex **4**, which has one less methylene unit, reveals that lengthening the chelation arm results in increased thermodynamic stability of the resulting Rh(II) complex. This phenomenon is presumably due to the increased ability of **5** to accommodate structural changes (lengthening of the Rh−P

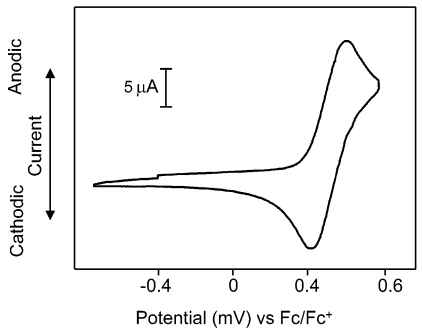

Figure 1. Cyclic voltammogram of **6** in CH_2Cl_2/0.1 M *n*-Bu_4NPF_6 using a Au working electrode, a Pt mesh counter electrode, and a Ag wire quasi-reference electrode at a scan rate of 400 mV/s. Ferrocene was used as an internal reference in a subsequent scan.

(13) Farrell, J. R.; Eisenberg, A. H.; Mirkin, C. A.; Guzei, I. A.; Liable-Sands, L. M.; Incarvito, C. D.; Rheingold, A. L.; Stern, C. L. *Organometallics* **1999**, *18*, 4856.
(14) Reike, R. D. *Aldrichimica Acta* **2000**, *33*, 52.

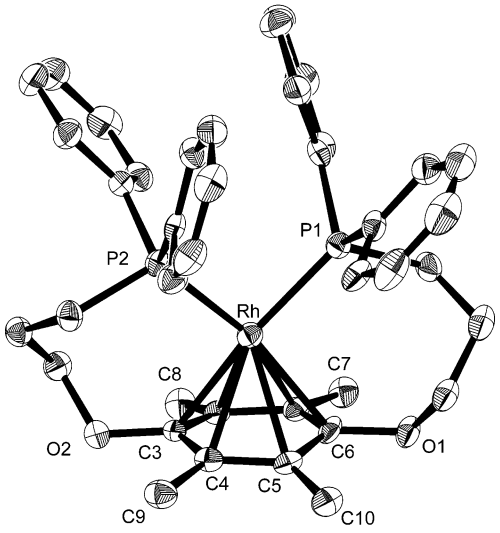

Figure 2. ORTEP diagram of **5**. Thermal ellipsoids are drawn at 50% probability, and counterions, hydrogen atoms, and lattice solvent are omitted for clarity. See Table 2 for selected bond distances and angles.

bonds and widening of the P−Rh−P angle) upon oxidation. The need for this type of flexibility has been demonstrated with related complexes.[4] The 90 mV decrease in $E_{1/2}$ in going from **5** to **6** is attributed to the increase in electron richness of the arene in **6**. Consistent with this conclusion, it has been shown that replacement of a single ether group with a methylene unit in an analogous two-legged piano-stool complex results in a 58 mV decrease in $E_{1/2}$.[4a]

Solid-State Characterization of Complexes 5 and 6. The structures of **5** and **6** were determined by single-crystal X-ray diffraction methods and can be compared with the known structure of **4** (Figures 2 and 3A; Tables 1 and 2).[13] Crystals of **5** suitable for X-ray diffraction analysis were grown by slow diffusion of benzene into a CH_2Cl_2 solution saturated with **5**. Similarly, crystals of **6** were grown by slow diffusion of pentane into a CH_2Cl_2 solution saturated with **6**. As with **4**, the Rh atoms in **5** and **6** are centered on the arene ring of the two-legged piano stool. The P−Rh−P bond angles for complexes **5** and **6** are smaller than that for **4** (**4**, 96.48(2)°; **5**, 93.28(5)°; **6**, 94.89(4)°), and the average Rh−P and Rh−arene bond distances in complex **4** are shorter than those in **5** and **6** (**4**, Rh−P_{av} = 2.2388 Å, Rh−arene = 1.83 Å; **5**, Rh−P_{av} = 2.2585 Å, Rh−arene = 1.88 Å; **6**, Rh−P = 2.2508 Å, Rh−arene = 1.87 Å). These differences are attributed to the lengthening of the tether arms in complexes **5** and **6** by one methylene unit as compared with **4**. Both durenyl moieties in **5** and **6** are nonplanar with average deviations of planarity of 0.0468 and 0.0387 Å, respectively. The arene rings in all three complexes adopt boat confirmations with two short and four long Rh−C bonds. The bow and stern of the boats are pointed toward the rhodium metal center and are formed by the carbon atoms connecting the tether arm to the arene ring (**5**, C(3) and C(6); **6**, C(1) and C(4)).

Synthesis and Characterization of Rh(II) complexes 5^+ and 6^+. Compounds **5** and **6** were chemically oxidized to their Rh(II) forms, 5^+ and 6^+, with AgX (X = BF_4 or PF_6) salts ($E_{1/2} \cong$ 650 mV/s vs Fc/Fc^+ in CH_2Cl_2)[15] and isolated as red-brown and brown solids, respectively. Compounds 5^+ and 6^+ have been characterized by ^1H and $^{31}P\{^1H\}$ NMR spectroscopy, mass spectrometry, elemental analysis, and EPR spectroscopy. Consistent with the formation of paramagnetic Rh(II) compounds, ^1H and $^{31}P\{^1H\}$ NMR spectroscopy of both complexes in CD_2Cl_2 exhibit broad, nearly featureless spectra. Although complex 5^+ is moderately stable in solution under an inert atmosphere, we were unable to grow suitable crystals for characterization by single-crystal X-ray diffraction analysis; disproportionation occurred during crystal growth (∼1 week) resulting in the formation of **5** and unidentified products. Complex 6^+ is indefinitely stable in the solid state in air and substantially more stable than 5^+ in solution, which allowed us to grow crystals suitable for single-crystal X-ray diffraction analysis.

Solid-State Characterization of 6^+. Single crystals of 6^+ suitable for an X-ray diffraction analysis were grown by slow vapor diffusion of diethyl ether into a CH_2Cl_2 solution saturated with 6^+ at 0 °C (Figure 3B; Tables 1 and 2). Comparison of the structures of **6** and 6^+ shows that they are remarkably similar with only a few notable differences. It was postulated that the ligand framework should be flexible enough to undergo two types of structural changes, namely, the lengthening of the Rh−P bonds and widening of the P−Rh−P angle, to stabilize the Rh(II) metal center upon oxidation of the Rh(I) complex **6**.[4a] Indeed, the Rh−P bonds in 6^+ are longer than those in **6** by about 0.1 Å (Rh−P_{av} = 2.3422 Å), which is consistent with a decrease in π-back-bonding between the phosphines and the metal that is expected upon oxidation. The P−Rh−P angle is slightly affected upon going from **6** to 6^+ (widens by ∼0.5°), which is attributed to the ligand having adopted a near ideal geometry prior to oxidation. In other words, ligands that constrain the P−Rh−P angle (e.g., 1,2-bis(diphenylphosphino)ethane) have led to less stable Rh(II) complexes.[4a]

In addition to the changes in the $Rh(PPh_2)_2$ unit upon oxidation, the Rh−arene interaction is perturbed as evidenced by the shortening of the Rh−centroid distance (0.03 Å) and three of the Rh−C bonds. Like its Rh(I) analogue, the arene ring in complex 6^+ adopts a boat conformation with the bow and stern of the boat being made up of C(19) and C(22). The average deviation from planarity is smaller in 6^+ (0.022 Å) than in **6** (0.033 Å), which is consistent with the tendency of arene rings in $17e^-$ two-legged piano-stool complexes to be more planar than analogous $18e^-$ complexes, which often adopt boat structures.[16] In contrast to complex **6**, the bow and stern of the boat-shaped arene in 6^+ consist of two longer bonds (Rh−C(19) and Rh−C(22)) making the boat point away from the rhodium center. The arene ring flip upon oxidation of **6** to 6^+ is accompanied by a rotation of the $Rh(PPh_2)_2$ unit about the metal−arene axis. The phosphine groups in the Rh(I) complex **6** are rotated clockwise (θ = 21°) out of the plane defined by Rh and the carbon atoms on the arene ring that attach the tethers, C(1) and C(4) (Figure

(15) Connelly, N. G.; Geiger, W. E. *Chem. Rev.* **1996**, *96*, 877.
(16) (a) Muetterties, E. L.; Bleeke, J. R.; Wucherer, E. J. *Chem. Rev.* **1982**, *82*, 499. (b) Radonovich, L. J.; Klabunde, K. J.; Behrens, C. B.; McCollor, D. P.; Anderson, B. B. *Inorg. Chem.* **1980**, *19*, 1221.

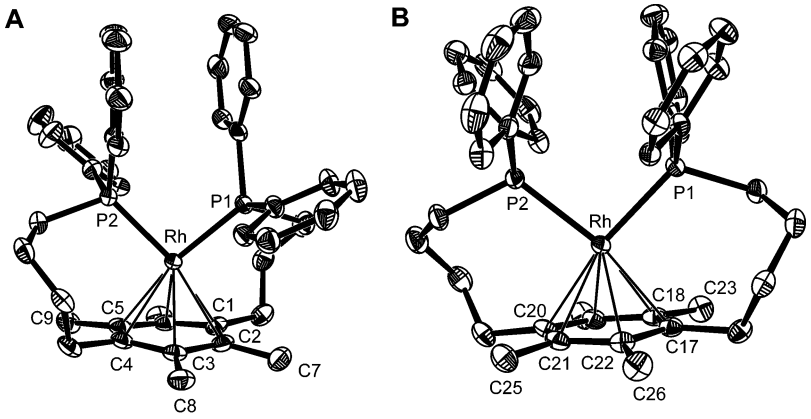

Figure 3. (A) ORTEP diagram of **6**. Thermal ellipsoids are drawn at 50% probability, and counterions, hydrogen atoms, and solvent molecules are omitted for clarity. See Table 2 for selected bond distances and angles. (B) ORTEP diagram of $\mathbf{6}^+$. Thermal ellipsoids are drawn at 50% probability, and counterions, hydrogen atoms, and solvent molecules are omitted for clarity. See Table 2 for selected bond distances and angles.

Table 2. Selected Bond Distances (Å) and Angles (deg) for **5**, **6**, and $\mathbf{6}^+$

complex **5**		complex **6**		complex $\mathbf{6}^+$	
Rh−P(1)	2.2532(13)	Rh−P(1)	2.2514(9)	Rh−P(1)	2.3381(7)
Rh−P(2)	2.2639(12)	Rh−P(2)	2.2501(10)	Rh−P(2)	2.3463(8)
Rh−C(6)	2.269(4)	Rh−C(1)	2.314(4)	Rh−C(17)	2.316(2)
Rh−C(1)	2.376(4)	Rh−C(6)	2.413(4)	Rh−C(18)	2.319(2)
Rh−C(2)	2.357(2)	Rh−C(5)	2.344(4)	Rh−C(19)	2.343(3)
Rh−C(3)	2.285(4)	Rh−C(4)	2.314(4)	Rh−C(20)	2.306(3)
Rh−C(4)	2.356(4)	Rh−C(3)	2.379(4)	Rh−C(21)	2.315(3)
Rh−C(5)	2.409(4)	Rh−C(2)	2.330(4)	Rh−C(22)	2.355(3)
Rh−arene	1.88	Rh−arene	1.87	Rh−arene	1.84
P(1)−Rh−P(2)	93.28(5)	P(1)−Rh−P(2)	94.89(4)	P(1)−Rh−P(2)	95.41(2)

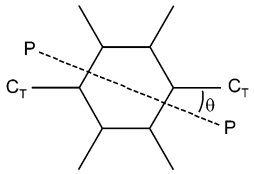

Figure 4. Representation of out of plane rotation of the phosphine groups (P) in complexes **6** and $\mathbf{6}^+$ where $\theta = 0$ is the plane defined by the carbon atoms of the arene ring that attach the methylene tethers (C_T: **6**, C(1) and C(4); $\mathbf{6}^+$, C(17) and C(22)) and the Rh center. θ represents the angle of rotation.

4). Upon oxidation of **6** to form the Rh(II) analogue, $\mathbf{6}^+$, the phosphine moieties shift closer to the tethered carbon atoms, C(17) and C(20), where $\theta = 15°$.

The deviations from planarity of the arene rings in complexes **4**−**6** and $\mathbf{6}^+$ are consistent with what has been observed with analogous η^6-arene−ML_2 complexes (e.g., $(\pi$-$C_6H_5CH_3)Ni(C_6F_5)_2$).[16,17] Molecular orbital diagrams for these reported complexes, which were constructed from extended Hückel molecular orbital calculations, reveal that the deviations from planarity are due to electronic effects. Specifically, to decrease the antibonding interaction between the metal−arene MO and the ligand orbitals either two or four bonds are lengthened to form the boat conformation. Although DFT calculations performed on PMe_2-substituted analogues of complexes **6** and $\mathbf{6}^+$ produce MO diagrams that are qualitatively consistent with those reported in the literature for analogous two-legged piano-stool complexes, we believe the difference in orientation of the arene ring between **4**−**6** and $\mathbf{6}^+$ cannot be due to electronic effects only. The methylene tethers in complexes **4**−**6** and $\mathbf{6}^+$ restrict the rotation of the $Rh(PPh_2)_2$ fragment about the metal−arene interaction. The ability for ML_2 fragments to adopt either a through-bond or through-atom configuration with the arene ring is the origin of the two different orientations (boat toward or away from metal) of the boat structure. In addition to the methylene tethers restricting rotation, the phenyl groups of the phosphine units sterically hinder rotation about the metal−arene axis. For these reasons, we believe the ring flip that accompanies the Rh(I) to Rh(II) conversion can be attributed to both steric and electronic factors.

EPR and Theoretical Studies. The paramagnetic d^7 Rh(II) metal centers were examined by X-band EPR spectroscopy. The frozen solution EPR spectrum of complex $\mathbf{5}^+$ displays a rhombic pattern with no resolved hyperfine splittings (Figure 5A, solid line). The best-fit computer simulation (Figure 5A, dashed line) gives the **g** tensor values and line widths of $g_1 = 2.390$ (85 MHz), $g_2 = 2.038$ (140 MHz), and $g_3 = 1.997$ (90 MHz). The frozen solution EPR spectrum of $\mathbf{6}^+$ (Figure 5B, solid line) appears to exhibit an axial pattern with no resolved hyperfine splittings; however, computer simulation of the experimental spectrum of $\mathbf{6}^+$ (Figure 5B, dashed line) requires a slight rhombic splitting of the g_z feature. The parameters that best simulate the experimental spectrum are $g_1 = 2.363$ (82 MHz), $g_2 = 2.0245$ (77 MHz), $g_3 = 2.0045$ (77 MHz).

The $g_{\|}$ value of 2.36 for complex $\mathbf{6}^+$ clearly indicates that the odd electron is in a substantially metal-centered orbital.

(17) (a) Albright, T. A.; Hoffmann, R.; Tse, Y.-C.; D'Ottavio, T. *J. Am. Chem. Soc.* **1979**, *101*, 3812. (b) Radonovich, L. J.; Koch, F. J.; Albright, T. A. *Inorg. Chem.* **1980**, *19*, 3373.

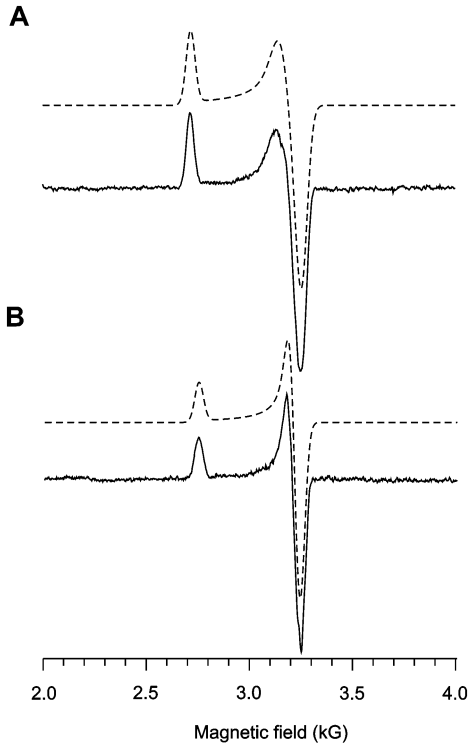

Figure 5. Frozen solution (solid lines) and simulated (dashed lines) EPR spectra of $\mathbf{5}^+$ (A) and $\mathbf{6}^+$ (B). Microwave frequency: $\mathbf{5}^+$, 9.105 GHz; $\mathbf{6}^+$, 9.090 GHz. Microwave power: $\mathbf{5}^+$ and $\mathbf{6}^+$, 20 mW. Modulation amplitude: $\mathbf{5}^+$ and $\mathbf{6}^+$, 5 G. Sweep time: $\mathbf{5}^+$ and $\mathbf{6}^+$, 4 min. Time constant: $\mathbf{5}^+$, 250 ms; $\mathbf{6}^+$, 125 ms.

Chart 1

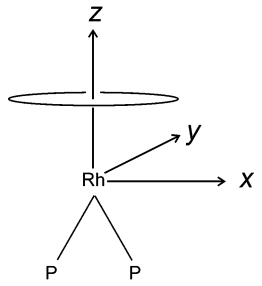

In agreement with this, using the axis system as defined in Chart 1, the DFT calculated structure of an analogue of complex $\mathbf{6}^+$ (phenyl rings are substituted with methyl groups) revealed a large metal contribution to the SOMO from the d_{yz} orbital (Figure 6); the calculation further gives the LUMO to be the d_{xz} orbital, which is consistent with reported rhodium(I) two-legged piano-stool complexes.[4a]

We undertook a single-crystal EPR experiment of complex $\mathbf{6}^+$ to substantiate the electronic structure determined by the

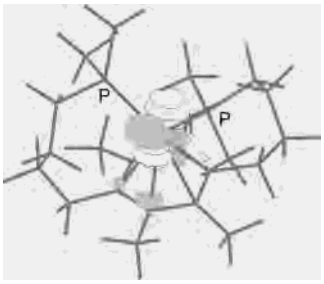

Figure 6. 0.05 e/au^3 isosurface of the SOMO of $\mathbf{6}^+$.

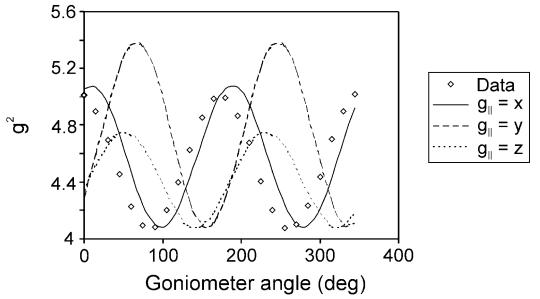

Figure 7. Angular variation of theoretical and experimental g^2 values versus goniometer angle where 0° corresponds to the $10\bar{1}$ face.

DFT calculations. There are four magnetically equivalent sites in the unit cell that give rise to only one EPR signal, which simplifies the analysis. Ignoring the slight rhombic splitting, we treat the **g** tensor as axial with $g_{||} = 2.36$ and $g_{\perp} = 2.02$. A single rotation with the magnetic field normal to the unique crystallographic (*b*) axis is sufficient to identify the molecular direction of $g_{||}$. A single crystal was mounted and indexed on a quartz fiber using Paratone and vacuum grease with the rotation axis coincident to the molecular *b* axis. EPR measurements were recorded every 15° over a 360° range while the crystal was rotated in the *ac* plane. The experimental g^2 value is compared to predicted g^2 values in which the $g_{||}$ direction is assumed to be either *x*, *y*, or *z* (Figure 7). The data best correspond to the assignment $g_{||} = g_x$, which is consistent with the simple ligand-field prediction for a d_{yz} ground state. As complex $\mathbf{5}^+$ has an EPR spectrum similar to that of $\mathbf{6}^+$, we take by analogy that the electronic structure of $\mathbf{5}^+$ is the same as that of $\mathbf{6}^+$.[18]

Reactivity of the Rh(I) Complex 6 and Rh(II) Complex $\mathbf{6}^+$ with Small Molecules. In addition to structurally and electronically characterizing the mononuclear Rh(I) and Rh(II) complexes **6** and $\mathbf{6}^+$, we have investigated their reactivities with small molecules. The η^6-arene moieties of other mononuclear and dinuclear two-legged piano-stool Rh(I) complexes have been shown to be substitutionally labile in the presence of small molecules such as CO and acetonitrile.[13,19] These small molecules bind more strongly to the Rh(I) metal centers, resulting in the displacement of the arene group and subsequent formation of square planar or trigonal bipyramidal bisphosphine complexes. Therefore, an important issue pertains to the effect of the chelating environment in **6** and $\mathbf{6}^+$ on the lability of the arene moieties in these complexes.

To address this issue, the reactivity of the Rh(I) piano-stool complex **6** with CO, *tert*-butyl isocyanide, and acetonitrile was initially studied. When a CD_2Cl_2 solution of **6** is charged with CO (1 atm), the Rh−arene interaction is broken, and the tricarbonyl *trans*-phosphine complex, [(η^1:η^1-1,4-bis[4-(diphenylphosphino)butyl]-2,3,5,6-tetramethylbenzene)-

(18) The observed $g_3 > g_e$ value for $\mathbf{6}^+$ and the lack of resolved hyperfine splittings both in $\mathbf{5}^+$ and $\mathbf{6}^+$ remain open questions that are being pursued by both advanced EPR spectroscopy (ENDOR and ESEEM) and DFT calculations.

(19) (a) Singewald, E. T.; Mirkin, C. A.; Levy, A. D.; Stern, C. L. *Angew. Chem., Int. Ed. Engl.* **1994**, *33*, 2473. (b) Singewald, E. T.; Shi, X.; Mirkin, C. A.; Schofer, S. J.; Stern, C. L. *Organometallics* **1996**, *15*, 3062.

Scheme 3

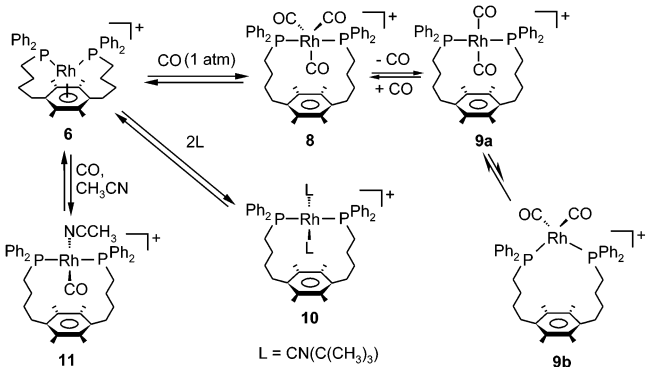

$Rh(CO)_3][PF_6]$, **8**, forms as the sole product (Scheme 3). The conversion of **6** to **8** was monitored by $^{31}P\{^1H\}$ NMR spectroscopy, which exhibited a downfield shift in the initial resonance associated with **6** (δ 28.0, $J_{Rh-P} = 204$ Hz) to a new resonance at δ 30.4 ($J_{Rh-P} = 72$ Hz). The latter resonance and coupling constant are diagnostic of a *trans*-bisphosphine five-coordinate complex with equatorial CO ligands and are consistent with our structural assignment for **8**.[13,19] The FT-IR spectrum of **8** exhibits three metal carbonyl bands at 2023 (s), 2034 (s), and 2091 (w) cm^{-1}, which is consistent with a trigonal bipyramidal metal complex with an asymmetric ligand environment. The asymmetry of the ligand splits the E′ mode yielding three νCO bands rather than the two typically observed for complexes with local D_{3h} symmetry. Splitting of the carbonyl bands due to asymmetric ligand environments has been observed in similar mononuclear rhodium(I) and cobalt(I) complexes.[20]

Although qualitatively similar reactivity has been well-documented for isostructural Rh(I) complexes (in particular, CO-induced arene displacement), the reaction of **6** with CO is significantly slower than for many of the related complexes studied thus far under comparable conditions.[13,19b] For example, the conversion of **6** to **8**, under an atmosphere of CO, takes over 20 days at room temperature whereas an analogous binuclear complex with a two-legged piano-stool geometry at each metal center quantitatively converts to the tris-CO adduct per Rh(I) center under an atmosphere of CO within 2 h.[13] The decrease in reactivity of **6** toward CO compared to similar mononuclear and dinuclear two-legged piano-stool type complexes is a direct result of the symmetric chelation of the η^6-arene group to the Rh center and the methyl substitution of the arene. In addition, there is another important electronic effect that stabilizes **6**. The HOMO in **6** is the d_{yz}, which bisects the P−Rh−P plane (*xz* plane) (Chart 1). The space-filling representation of the theoretical model for **6** indicates that the metal center is exposed along the filled HOMO (d_{yz}) whereas the LUMO (d_{xz}, along the Rh−P bonds) is protected by the ligand framework, which inhibits the substitution reaction.

Interestingly, the substitution reaction of the Rh(II) complex $\mathbf{6}^+$ with CO occurs dramatically faster than for the analogous Rh(I) complex **6**. It is well-known that 17-electron organometallic complexes often undergo substitution reactions at faster rates than their 18-electron counterparts.[21] Saturating a CH_2Cl_2 solution of $\mathbf{6}^+$ with CO and heating in a sealed NMR tube results in a yellow solution that is EPR silent. The $^{31}P\{^1H\}$ NMR spectrum, on the other hand, exhibits a doublet at δ 30 ($J_{Rh-P} = 72$ Hz), which is identical to the doublet in the spectrum for CO-substituted Rh(I) complex **8** (Scheme 4). FT-IR spectroscopy confirmed the formation of **8** via the reduction of the Rh(II) complex $\mathbf{6}^+$. ^{13}CO-labeling studies show a new resonance at δ 125 in the $^{13}C\{^1H\}$ NMR spectrum upon reaction of ^{13}CO with $\mathbf{6}^+$, which is consistent with the formation of $^{13}CO_2$. The $^{13}C\{^1H\}$ NMR and the $^{31}P\{^1H\}$ NMR spectra of the ^{13}CO analogue of **8** taken at −70 °C exhibited a doublet of triplets at δ 184.6 ($J_{C-Rh} = 64$ Hz, $J_{C-P} = 12$ Hz) and a doublet of quartets at δ 30 ($J_{Rh-P} = 204$ Hz; $J_{P-P} = 13$ Hz), respectively, verifying the binding of three CO moieties per rhodium center. A similar reduction of Rh(II) has been observed with $[PBzPh_3]_2[Rh(C_6Cl_5)_4]$ after bubbling of CO through a CH_2Cl_2 suspension to yield a Rh(I) adduct, but the oxidation product was not identified.[22] Also, Dunbar and co-workers have reported the formation of Rh(I) and Rh(III) disproportionation products when CO is reacted with $[Rh(tmpp)_2]^{2+}$ (tmpp = tris(2,4,6-trimethoxyphenyl)phosphine).[23] Since only one compound is observed in the $^{31}P\{^1H\}$ NMR spectrum of the product mixture formed from the reaction between $\mathbf{6}^+$ and CO, a simple two-component disproportionation reaction has been ruled out.

Scheme 4

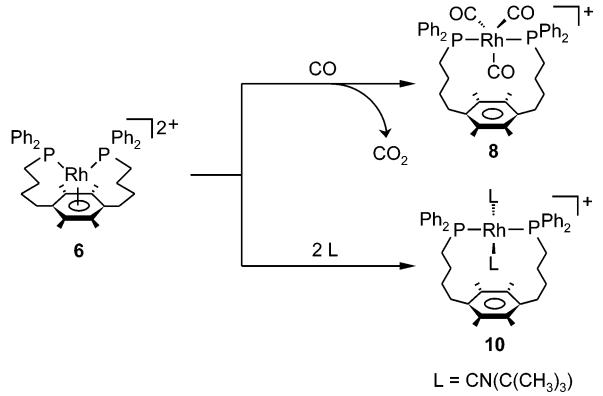

To increase the rate of formation of **8**, a CD_2Cl_2 solution of complex **6** in a sealed NMR tube was heated at 51 °C under an atmosphere of CO for 3 days. Instead of observing only resonances due to **8**, the $^{31}P\{^1H\}$ NMR spectrum exhibited a new doublet at δ 23.9 ($J_{Rh-P} = 121$ Hz). On the basis of the similarity in coupling constant and chemical shift with data for analogous *trans*-phosphine complexes,[19b] this new product was determined to be [*trans*-(η^1: η^1-1,4-bis[4-(diphenylphosphino)butyl]-2,3,5,6-tetramethylbenzene)Rh-

(20) (a) Alvarez, M.; Lugan, N.; Donnadieu, B.; Mathieu, R. *Organometallics* **1995**, *14*, 365. (b) Alvarez, M.; Lugan, N.; Mathieu, R. *Inorg. Chem.* **1993**, *32*, 5652. (c) Yagupsky, G.; Brown, C. K.; Wilkinson, G. *J. Chem. Soc. A* **1970**, 1392.

(21) Trogler, W. C. In *Organometallic Radical Processes*; Trogler, W. C., Ed.; Elsevier: Amsterdam, 1990; Vol. 22, pp 306−337.

(22) García, M. P.; Jimenez, M. V.; Cuesta, A.; Siurana, C.; Oro, L. A.; Lahoz, F. J.; Lopez, J. A.; Catalan, M. P. *Organometallics* **1997**, *16*, 1026.

(23) Haefner, S. C.; Dunbar, K. R.; Bender, C. *J. Am. Chem. Soc.* **1991**, *113*, 9540.

$(CO)_2][PF_6]$, **9a**, the bis-CO analogue of **8**. The ^1H NMR spectrum of the solution indicated that a very small amount of **8** was also present in solution. Complete conversion to **9a** was never observed, even after prolonged heating (14 days). Cooling of the reaction mixture containing predominantly **9a** (**8** is undetectable by $^{31}P\{^1H\}$ NMR) to room temperature resulted in a decrease in **9a** and increase in **8** (after 5 days, **8**:**9a** ratio = 2:1). The product ratio of this mixture can be repeatedly affected by changes in temperature in a reversible manner. While prolonged heating of the mixture of **8** and **9a** results in the formation of the tris-CO product and one bis-CO product, monitoring of the reaction by $^{31}P\{^1H\}$ NMR spectroscopy at an early stage shows the appearance of a second upfield resonance δ 25.3 (J_{Rh-P} = 105 Hz) assigned to the *cis*-bis-CO adduct, **9b**. Comparison with literature values of analogous complexes supports this assignment.[20a,b] Due to overlapping resonances, it is difficult to get reliable quantitative integration data in the ^1H NMR spectrum and to discern the assignment of the FT-IR spectrum of the reaction mixture. Qualitatively, the reaction involving **8** and **9a** can be described as a mildly endothermic process that favors product **9a** at higher temperatures.

Complex **6** also reacts with *tert*-butyl isocyanide (51 °C, 10 days) through an arene displacement reaction to yield [(η^1:η^1-1,4-bis[4-(diphenylphosphino)butyl]-2,3,5,6-tetramethylbenzene)Rh$(CNC(CH_3)_3)_2][PF_6]$, **10**. This complex exhibits a doublet in its $^{31}P\{^1H\}$ NMR spectrum at δ 23.6 (J_{Rh-P} = 123 Hz), which is consistent with the formation of a square planar Rh(I) complex with *trans*-phosphine atoms as observed in similar *trans*-nitrile *trans*-phosphine macrocyclic complexes. The FT-IR spectrum exhibits a characteristic ν_{NC} stretch at 2135 cm^{-1}. The reaction between two isocyanide molecules and complex **6** to form **10** was also confirmed by mass spectrometry (M^+ = 883.1). As with CO, the 17-electron Rh(II) complex $\mathbf{6}^+$ reacts faster in the presence of 2 equiv of *tert*-butyl isocyanide but still forms the same product as that formed with the reduced complex **6**. Indeed, the reaction is complete within 24 h with the only spectroscopically observable ($^{31}P\{^1H\}$ NMR and FT-IR) metal-containing complex being **10** (Scheme 4). The reducing agent was not identifiable for this reaction. A similar reduction of mononuclear Rh(II) to Rh(I) in the presence of *tert*-butyl isocyanide has been observed by Wilkinson and co-workers with $Rh(2,4,6\text{-}Pr^i_3C_6H_2)_2(tht)_2$ (tht = tetrahydrothiophene), which occurs via hydrogen abstraction from the solvent.[24] In addition, a Rh(II) porphyrin, Rh(II) TMP (TMP = tetrakis(2,4,6-trimethylphenyl)porphyrinato), reacts with $CNCH_3$ to form the Rh(I) adducts (TMP)RhCN and CH_3Rh(TMP).[25] If hydrogen abstraction was occurring to form a Rh(I) adduct, one would not expect to see the clean formation of product **10**.

Finally, complex **6** reacts with CO in the presence of CH_3CN in CD_2Cl_2 to yield the cationic Rh(I) complex [(η^1:η^1-1,4-bis[4-(diphenylphosphino)butyl]-2,3,5,6-tetramethylbenzene)-Rh(CO)$(CH_3CN)][PF_6]$, **11**. This reaction occurs after 18 days at room temperature. Complex **11** was characterized by ^1H and $^{31}P\{^1H\}$ NMR spectroscopy, mass spectrometry, and an X-ray diffraction analysis. The $^{31}P\{^1H\}$ NMR spectrum exhibits a doublet at δ 27.2 (J_{Rh-P} = 97 Hz) characteristic of a *trans*-phosphine square planar complex with a CO ligand trans to an acetonitrile ligand. The FT-IR spectrum exhibits characteristic stretches at 1976 and 2218 cm^{-1} (ν_{CO} and ν_{MeCN}, respectively). The reaction between $\mathbf{6}^+$ and acetonitrile resulted in decomposition and no identifiable products.

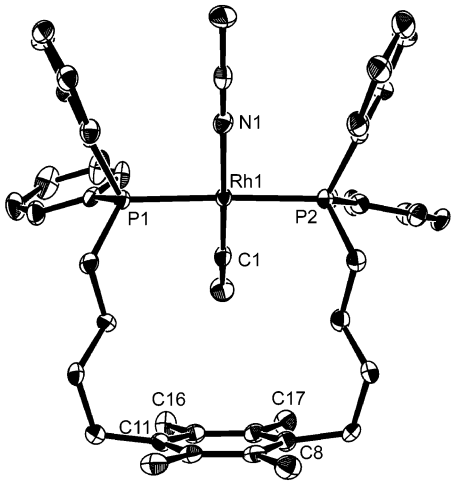

Figure 8. ORTEP diagram of **11**. Thermal ellipsoids are drawn at 50% probability, and counterions, hydrogen atoms, and solvent molecules are omitted for clarity. Selected bond distances (Å) and angles (deg): Rh−arene(centroid) = 5.636, Rh(1)−P(1) = 2.3373(12), Rh(1)−P(2) = 2.3332(12), Rh(1)−C(1) = 1.819(5), Rh(1)−N(1) = 2.054(4), P(1)−Rh(1)−P(2) = 175.45(4).

The observed rates of reactions involving **6** and $\mathbf{6}^+$ with CO and *tert*-butyl isocyanide, respectively, suggest that, in the case of the 17-electron complex $\mathbf{6}^+$, ligand substitution takes place prior to electron transfer. Otherwise, in the case of $\mathbf{6}^+$, one would expect to observe formation of some reduced **6**, yet this has not been observed under the conditions explored thus far. The facilitated conversion of $\mathbf{6}^+$ to **8** as compared with **6** to **8** is likely due to the ability of the 17-electron complex to support the coordination of an additional ligand through an associative pathway to form a 19-electron complex. Subsequent reduction and then arene displacement through the addition of two more CO ligands leads to product **8**. In the case of **6**, ligand displacement through ring slippage or phosphine dissociation must occur prior to CO uptake.

Solid-State Characterization of 11. Single crystals of **11** suitable for an X-ray diffraction analysis were grown by slow diffusion of pentane into a CH_2Cl_2 solution saturated with **11** at room temperature (Figure 8; Table 1). Upon displacement of the arene ring, the Rh−arene centroid distance becomes 5.636 Å. The Rh−P average bond length of 2.3353 Å is slightly longer than the Rh−P average bond lengths for the piano-stool complex **6**, 2.250 Å, and compares well with bond length data for similar square planar binuclear complexes with trans CO/CH_3CN groups at each metal center (2.3265 and 2.335 Å).[13] The geometry about the Rh(I) metal center is slightly distorted square planar with a P(1)−Rh-

(24) Hay-Motherwell, R. S.; Koschmieder, S. U.; Wilkinson, G.; Hussain-Bates, B.; Hursthouse, M. B. *J. Chem. Soc., Dalton Trans.* **1991**, 2821.
(25) Wayland, B. B.; Sherry, A. E.; Bunn, A. G. *J. Am. Chem. Soc.* **1993**, *115*, 7675.

(1)−P(2) angle of 175.45(4)°. The CO moiety is pointed toward the arene between carbon atoms C(16) and C(17) where the CO deviates from the plane made up of C(8)−Rh−C(11) by 41.9°. Major differences between the arene-bound complex **6** and the unbound complex **11** are the orientation of the phosphine tethers with respect to the arene ring and the conformation of the arene ring. The P(1)−Rh-(1)−P(2) triad lies in the same plane as C(8)−Rh(1)−C(11), which are the carbon atoms attached to the tether arms, instead of twisting about the arene ring. Due to the lack of metal binding, the arene ring is planar rather than distorted in a boat orientation as in **6**.[16a]

Conclusions

This manuscript reports the synthesis, characterization, and reactivity of Rh(I) and Rh(II) two-legged piano-stool monomers. The stabilizing effects of the ligands are demonstrated and reveal three factors that increase the stability of mononuclear Rh(II) in this geometry: (1) tether arms containing four spacer units connecting the phosphine groups to the arene ring; (2) electron richness of the arene, which is increased by replacing ether moieties attached to the arene ring with methylene groups; and (3) symmetrically substituted arene rings to maximize chelation. The ligand framework kinetically stabilizes the unusual oxidation state due to the increased steric bulk about the metal center by inhibiting dimerization and reaction with solvent and other small molecules. In general, for the reactivity studied herein, the chemistry of the Rh(II) forms of these two-legged piano-stool complexes parallels that for the Rh(I) forms, but occurs at accelerated rates. This is believed to be due to the ability of the Rh(II) complexes to support associative reaction pathways prior to reaction, which facilitates ligand substitution.

Acknowledgment. C.A.M. acknowledges AFOSR and NSF for support of this research. F.M.D. acknowledges the Illinois Minority Graduate Incentive Program for a predoctoral fellowship. C.A.M. and F.M.D. acknowledge Charlotte Stern for X-ray data collection and analysis of complex **5**. P.E.D. acknowledges Professor Brian M. Hoffman for funding (NSF MCB-9904018 and NIH HL-13531) and helpful discussions, and Mr. Clark E. Davoust for technical support. The University of Delaware acknowledges the NSF for their support of the purchase of the CCD-based diffractometer (CHE00091968).

Supporting Information Available: Tables of crystallographic data for complexes **5**, **6**, $\mathbf{6}^{+}$, and **11**, and atomic coordinates for the DFT calculated structures analogous to complexes **6** and $\mathbf{6}^{+}$. X-ray data available as the CIF files for complex **11**. The CIF files for **5**, **6**, and $\mathbf{6}^{+}$ can be obtained from manuscript OM020248S.[3] This material is available free of charge via the Internet at http://pubs.acs.org.

IC0204981